INFECTION AND IMMUNITY, Aug. 2005, p. 4895–4904 Vol. 73, No. 8
0019-9567/05/$08.00+0 doi:10.1128/IAI.73.8.4895–4904.2005

Comparison of *Helicobacter pylori* Virulence Gene Expression In Vitro and in the Rhesus Macaque

Jenni K. Boonjakuakul,[1,2]* Don R. Canfield,[3] and Jay V. Solnick[1,2,4]

Departments of Medical Microbiology and Immunology[1] and Internal Medicine,[2] California National Primate Research Center,[3] and Center for Comparative Medicine,[4] University of California at Davis, Davis, California 95616

Received 24 September 2004/Returned for modification 27 December 2004/Accepted 23 March 2005

We used a quantitative real-time reverse transcriptase PCR assay to measure the transcript abundance of 46 known and putative *Helicobacter pylori* virulence genes, including 24 genes on the Cag pathogenicity island. The expression profile of *H. pylori* cells grown in vitro was also compared to expression in vivo after experimental infection of rhesus macaques. Transcript abundance in vitro (mid-log phase) ranged from about 0.004 (*feoB* and *hpaA*) to 20 (*ureAB*, *napA*, and *cag25*) copies/cell. Expression of most genes was repressed during the transition from logarithmic- to stationary-phase growth, but several well-characterized *H. pylori* virulence genes (*katA*, *napA*, *vacA*, and *cagA*) were induced. Comparison of results in the rhesus macaque with similar data from humans showed a strong correlation ($r = 0.89$). The relative in vivo expression in the rhesus monkey was highly correlated with in vitro expression during mid-log ($r = 0.89$)- and stationary ($r = 0.88$)-phase growth. Transcript abundance was on average three- to fourfold reduced in vivo compared to in vitro during mid-log phase. However, when compared to stationary phase, increased expression in vivo was observed for 6 of 7 genes on a contiguous portion of the pathogenicity island, several of which are thought to encode the *H. pylori* type IV structural pilus and its accessory proteins. These results suggest the possibility that some genes encoding the *H. pylori* type IV structural pilus and accessory proteins may form an operon that is induced during growth in vivo.

Helicobacter pylori is a human pathogen that infects nearly half the world's population and produces a chronic infection that can lead to gastric and duodenal ulcers, gastric cancer, and B-cell mucosa-associated lymphoid tissue lymphoma (40). While most infected individuals show no signs or symptoms, approximately 10 to 15% will develop *H. pylori*-associated disease. More than half of the *H. pylori* strains found in the United States carry a 37-kb Cag pathogenicity island (PAI), which is more often found in isolates from patients with peptic ulcer disease, gastric cancer, or gastric lymphoma than in those with asymptomatic infection (2, 12). The Cag PAI genes encode a type IV secretion system required for transport of CagA (*c*ytotoxin *a*ssociated *g*ene) across the host cell membrane (8, 29, 33). Once inside the host cell, CagA is tyrosine phosphorylated, after which it interrupts host signal transduction (24) and induces a rearrangement of the actin cytoskeleton (33, 34). Most of the genes required to translocate CagA are also required to induce gastric epithelial cells to produce interleukin-8 (IL-8), which promotes inflammation by recruitment of polymorphonuclear leukocytes to the gastric epithelium (7, 20). Other gene products that are recognized to have an important role in *H. pylori* pathogenesis include urease (18), flagella (31), vacuolating cytotoxin (27), and a large family of outer membrane proteins, some of which function as adhesins (5, 44).

A further understanding of *H. pylori* pathogenesis requires analysis of the relative expression and conditions of expression for the Cag PAI and other major virulence determinants. Such an analysis may lead to the identification of bacterial factors that play a role in development of disease and help us to understand why some strains cause disease while others do not. It may also provide guidance for selection of drug targets or vaccine candidates, since most bacteria express virulence factors in a carefully regulated fashion. Although gene regulation by classical, two-component systems is probably less common in *H. pylori* than in organisms with an environmental niche as part of their life cycle, other methods of regulation, such as phase variation (45), are likely important. Since it is impossible to fully mimic in vitro the environmental conditions of infection in the host, it will be important to study in vivo expression directly in a relevant animal as well as in culture.

The rhesus monkey model is a relevant and tractable system for the study of *H. pylori* pathogenesis (15). Socially housed animals are naturally infected with *H. pylori* isolates that are nearly identical to human isolates (14, 16, 38). Infection is characterized by chronic gastritis and infiltration of polymorphonuclear leukocytes. Some infected monkeys develop atrophic gastritis, which is the histological precursor to gastric adenocarcinoma (15). Derivation of specific-pathogen (*H. pylori*)-free macaques by isolating them at birth provides a ready source of animals for experimental infection (37). The rhesus monkey model therefore provides an opportunity to investigate *H. pylori* gene expression after experimental infection under carefully controlled conditions.

In this study we describe the use of quantitative real-time reverse transcriptase PCR (qRT-PCR) to analyze gene expression from bacterial cells grown in vitro and from small amounts of bacterial RNA recovered from gastric biopsy specimens of experimentally infected macaques. Expression levels of 46

* Corresponding author. Present address: Department of Medicine, Division of Infectious Disease, 513 Parnassus Avenue, HSE 418/Box 0654, University of California, San Francisco, San Francisco, CA 94143. Phone: (415) 502-5731. Fax: (415) 476-9364. E-mail: jennib@medicine.ucsf.edu.

TABLE 1. Genes and primer pairs selected for real-time RT-PCR

Category	Gene	HP no.[a]	Function	Forward primer	Reverse primer
Urease	*ureA*	HP0073	Structural subunit of urease enzyme	GAAGACATCACTATCAACGAAGGCAA	GTTACCGCCAATGTCAATCAA
	ureB	HP0072	Structural subunit of urease enzyme	CAATCCAACAACCCTAGCAAA	CCACCAGCAGTTACGATCAAA
	ureG	HP0068	Urease accessory gene	AACGCGCCACATGTCAAA	GCCTCCGCTTTCAATCAA
	ureI	HP0071	pH-dependent urea transporter	GGGTTAACCAAAGTCGATCCTAAA	ATAGCCGCATACAAGTAGGTGAA
	nixA	HP1077	High-affinity nickel transporter	GGATCACATCGCTTGCATAGATAA	GAATAATCGCATTCAATAGCCCTATAA
Outer membrane proteins	*omp11*	HP0472	Outer membrane protein HorE	GCTATGGCCCTTATAACAGCAA	GAGACCTAGAGCGAATTTATCCAA
	omp19 (*babB*)	HP0896	Unknown	GCAAGGGATAATCTAGGCTCAA	CATGTCCTGGCTCATAATACGAA
	omp24	HP1313	Outer membrane protein HorI	GCATTCAGCACAACTCTAGCAA	CCATATAAGTGCCGTAAGTGGAAA
	omp28 (*babA*)	HP1243	ABO blood group adhesin	GCACCCTAAACACCCTTATCAAA	ATACCCTGGCTCGTTGTTGAA
Iron	*feoB*	HP0687	Iron transport protein	CTTCACCACTGAAGAAAAGGTTACTAA	ATAAAGCCTGACAATTTCGTCTAATAA
	fur	HP1027	Ferric uptake regulator	CGCATTCTATCCGCCAAA	CTTACCGCAATGCAAACAAA
	napA	HP0243	Bacterioferritin; neutrophil-activating protein	ATGTGCATAAAGCCACTGAAGAA	GATCGCTTCGGATAAAGTGACTAA
Motility	*fliI*	HP1420	Flagellar export protein ATP synthase	TGGTGGTGGTGGCAGAAA	GCAAGTCAAAAGCCCATCAA
	fliP	HP0685	Flagellar basal body protein	TCTTACACCGAAGCGTTTGAA	CAAGTAGAGTAAAAAGCCGATTTGAA
	flgE	HP0870	Flagellar hook protein	ATCGCTACCGCACCCTATAA	CCCTTGCGAGTCAAAAAGAA
	hpaA	HP0797	Component of flagellar sheath	AGAGTATGAAAACAAATTCAAGAATCAA	AAACCCCTTCCATTTTATCCAA
	cheY	HP1067	Chemotactic response regulator	GTAGATGATAGCTCAACTATGAGGAGAA	TCATTTCAGGCATGTTCCAA
Miscellaneous	*katA*	HP0875	Catalase	GCGGCGTTTGACAGAGAA	TTTGATCGCATCACGGATAA
	sodB	HP0389	Superoxide dismutase	GCGGAGGCGTGTTCAATAA	TCCAACCAGAGCCAAACAAA
	comB8	HP0038	Competence	AACCACCAAGAAAAGCATTTAGAA	GGTTTAACACATACGCCCCAA
	nolK	HP0045	O-antigen biosynthesis, GDP-fucose synthetase	GGATGCACACCGCTAAATTAAA	TCACAAACACGCCCTTATAGTCTAA
	vacA	HP0887	Vacuolating cytotoxin	CACCCACTTGATTATTCACTCTTAAA	CCACCCAATAACACGCAAA
Cag PAI	*cag1*	HP0520	Unknown	GCTATGGGGATTGTTGGGATAA	GCTTCAGTTGGTTCGTTGGTAA
	cag3	HP0522	IL-8 induction and CagA translocation	GACACCTTGAATGTGAATGACAAA	GTTGTAATACCCATTGACTTGCTCTAA
	cag5	HP0524	CagA translocation	CGGACTAGAGATATAGGAGCGAATAA	GCCACGCCTGCCTACAA
	virB11	HP0525	ATPase: IL-8 induction and CagA translocation	CCTCTAAGGCATGCTACTGAAGAA	TCGCTAAATTGCTGCTCAAAA
	cag6	HP0526	Unknown	GAAAGCACGATCAAAAATGAACTAA	CAGATAAGAAGCCACTAGGTCTGAA
	cag7	HP0527	IL-8 induction and CagA translocation	AAGTCAGAAGAAATAACTGACGACTCTAA	TCACGATAAGAACAGCGACTACAA
	cag8	HP0528	IL-8 induction and CagA translocation	GAATTTTAATCGTGGTAGGGTGAA	TTATTGAAACCTGTTGTGATGTAAGAA
	cag9	HP0529	IL-8 induction and CagA translocation	TCTCATTGTTCCTAATTGGTTGAAA	CTTGTGGCTAATGGTGTGCTAA
	cag10	HP0530	IL-8 induction and CagA translocation	AACGAAGAAGTCTTGATTGATGAAA	CTGTGTATCGATCAATGCCATAA
	cag11	HP0531	IL-8 induction and CagA translocation	CACCTAGCAACTCACAGAGCAA	CCCACCCATACACAATCCTAA
	cag12	HP0532	IL-8 induction and CagA translocation	TGTTTTAATCGGTGCGACAA	GACCGTAATCTTTTTAGAATGGTGAA
	cag13	HP0534	Unknown	AATAACATGCGAAAACTCTTCTCAA	CTCCATAGTCTCACTCTCAAGCAA
	cag14	HP0535	Unknown	ACGCATTAGAGATCCGAACAA	CCATTCTTCAACACTTCTGCCATAA
	cag15	HP0536	Unknown	CAAACATTCTTTCAACAAACATTTAGATAA	GAAACGAGTAGCAAAAGATAAGTAGTGTAA
	cag16	HP0537	IL-8 induction and CagA translocation	GAAGAAGTGGCTGCAAAAGAA	CATAGGCATAAGGGTTAGGAAGAA
	cag17	HP0538	Unknown	TCAAAGACATGACGACGAAGAA	GCTCTTGCCCTATCATTTCGTAA
	cag18	HP0539	IL-8 induction and CagA translocation	CCAACCAACAAGTGCTCAAAAA	TCAATAACGCTAAATCTCCTCTCAA
	cag19	HP0540	CagA translocation	GACTTTTTGTGGTTTGTCTCTGAA	CGCCAAGCAAGATGTCTGAA
	cag20	HP0541	IL-8 induction and CagA translocation	GCTGCTAACCAACAATACAACCAA	CTAAGATACCGCTCATCATTTCAA
	cag21	HP0542	CagA translocation	GGGGCTTGTTTCTAGAGATCAACTAA	GAAAGGATTGTTTGGACCGTAA
	cag22	HP0543	CagA translocation	TTTATGTTTATGCTTACTTCATGCTAGAA	CGCTCATATCAATCTGAATCCAA
	cag23	HP0544	IL-8 induction and CagA translocation	GCTAGTCATAGAGCAAGAGGTTCAAAA	CACAATAACAATCGCTACAATCAAA
	cag25	HP0546	IL-8 induction and CagA translocation	CAAGAATCACTGACAGCTACAAGAA	ATACCGCCTGCCACCGCTAA
	cag26 (*cagA*)	HP0547	Immunodominant antigen; delivered into epithelial cells by a type IV secretion system	TTAACCCGCAGCAATTTATCAA	AGCTTTTTATGGAAGAACCTGTATCAA
Standard	16S		16S ribosomal RNA	GGAGTACGGTCGCAAGATTAAA	CTAGCGGATTCTCTCAATGTCAA

[a] *H. pylori* gene designation (see reference 44).

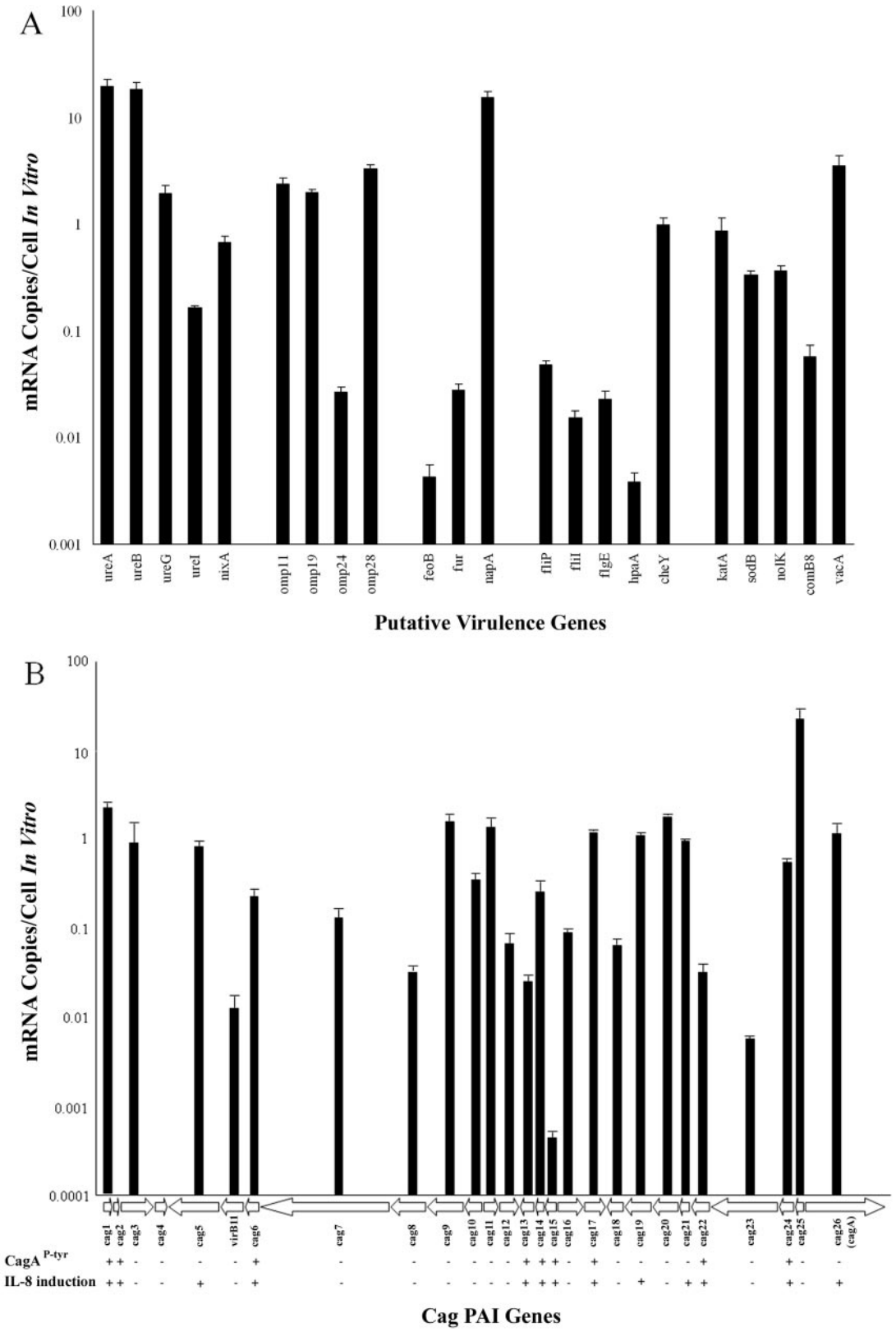

FIG. 1. In vitro expression (mRNA copies/cell) measured during the mid-logarithmic phase of growth (15 h; OD_{600}, 1.0). (A) Putative virulence genes. Genes are grouped according to similar functions (Table 1). (B) Cag pathogenicity island genes. Arrows represent the directions of the open reading frame. Plus and minus signs indicate whether a nonpolar deletion mutant in the respective PAI gene shows the phenotype of IL-8 induction or CagA tyrosine phosphorylation according to published data (20).

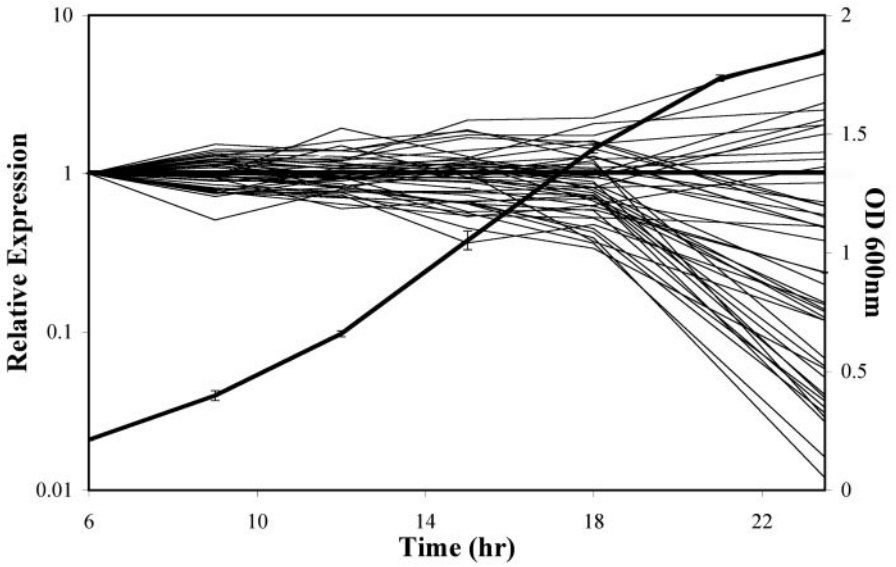

FIG. 2. Change in expression relative to time point 1 (6 h; OD_{600}, 0.2) for putative virulence genes and genes on the Cag PAI. Fine lines (*y* axis, left) represent individual genes whose relative mRNA copies per cell have either increased or decreased at each time point. The bold line (*y* axis, right) is the growth curve (mean OD_{600}) for *H. pylori* grown in duplicate liquid cultures. Relative expression levels fluctuate over the growth curve, with the most significant changes seen between 18 h (OD_{600}, 1.4) and 23.5 h (OD_{600}, 1.8), specifically as the growth is exiting logarithmic phase and entering stationary phase. The horizontal bold line drawn at 1.0 (*y* axis, left) shows expression equivalent to that at time point 1.

known or putative virulence genes were analyzed, which provides a transcript profile of gene expression during in vitro growth and during acute infection in the rhesus monkey.

MATERIALS AND METHODS

Bacterial strain and culture. *H. pylori* J166 contains a functional Cag PAI and the s1m1 allele of the *vacA* cytotoxin (39). Recent studies by us (39) and others (15) showed that *H. pylori* J166 preferentially colonizes rhesus monkeys. Plate-grown bacteria were cultivated on brucella agar (Difco Laboratories, Detroit, MI) containing 5% bovine calf serum (GibcoBRL, Gaithersburg, MD) supplemented with TVPA (trimethoprim, 5 mg/liter; vancomycin, 10 mg/liter; polymixin B, 2.5 IU/liter; amphotericin B, 4 mg/liter; all from Sigma, St. Louis, MO) and incubated at 37°C in an atmosphere that contained 5% CO_2. For liquid cultures, bacteria were grown in brucella broth containing 5% bovine calf serum with TVPA and incubated at 37°C with 5% CO_2 and gentle rotation at 60 rpm. Duplicate cultures were inoculated to an optical density at 600 nm (OD_{600}) of 0.05 with an overnight starter culture. OD_{600} was determined serially for each culture from 6 to 23.5 h after inoculation.

Animals. Five specific-pathogen-free rhesus macaques (two males and three females) between the ages of 3 to 4 years were located at the California National Primate Research Center (CNPRC), which is accredited by the Association for the Assessment and Accreditation of Laboratory Animal Care. All animals were confirmed to be free of *H. pylori* and "*Candidatus* Helicobacter heilmannii" (30) according to protocols described previously (37). Monkeys were housed indoors in separate cages throughout the course of the experiment. All procedures were approved by the CNPRC Research Advisory Committee and by the University of California, Davis, Chancellor's Animal Use and Care Administrative Advisory Committee.

Animal inoculations. A 50-ml liquid culture of *H. pylori* J166 was cultivated as above for 19 h to an OD_{600} of approximately 0.2. The culture was centrifuged and resuspended in fresh brucella broth to an OD_{600} of 1.0. Each monkey was inoculated orogastrically with 7.5×10^8 CFU/1.5 ml. The inoculum was examined by Gram stain, urease, and oxidase tests to ensure a pure culture of *H. pylori*.

Biopsies and quantitative cultures. Each monkey was biopsied at 1 week and 1, 2, 3, 4, and 6 months postinoculation (p.i.) using a pediatric gastroscope (Pentax FG-16X) with a 1.8-mm biopsy forceps. The procedure was performed under ketamine anesthesia (10 mg/kg of body weight intramuscularly) after an overnight fast. Eight antral biopsy specimens were collected from the stomach during each endoscopy. Six antral biopsy specimens were individually placed immediately in 200 μl Trizol (GibcoBRL) and put on ice. Two antral biopsy specimens were placed in 250 μl brucella broth for quantitative culture. Biopsy specimens were homogenized with a sterile glass rod before plating and RNA extractions. The 2 antral biopsy specimens in brucella broth were serially diluted, plated onto brucella agar supplemented with 5% bovine calf serum and TVPA, and incubated at 37°C with 5% CO_2 for 5 to 6 days. *H. pylori* colonies were identified in the conventional manner by colony morphology, microscopy, and biochemistry. CFU were counted and CFU/g of tissue were determined for each monkey. Individual isolates were passed and frozen at −80°C in brucella broth containing 20% (vol/vol) glycerol.

RNA extraction. At each OD_{600} determination, 2-ml aliquots were removed from the liquid cultures and centrifuged in a table top Microfuge for 30 s. The supernatant was removed, and 1 ml of Trizol was immediately added. Samples were vortexed, and RNA was extracted according to the manufacturer's directions. RNA was treated with DNase I (Roche Applied Science, Mannheim, Germany), purified using an RNeasy clean up kit (QIAGEN, Inc., Valencia, CA), and suspended in molecular biology grade water (BioWhittaker, Rockland, ME) at a concentration of 20 ng/μl. Samples were stored at −80°C prior to analysis. Total RNA was extracted from the six antral biopsy specimens using the Trizol protocol according to the manufacturer's instructions. RNA was treated with DNase I and purified using an RNeasy clean up kit. Purified RNA was suspended in 200 μl molecular biology grade water (BioWhittaker), diluted 1:5, and stored at −80°C prior to analysis.

DNA fingerprinting. Repetitive extragenic palindromic PCR (Rep-PCR) was used to type strains recovered from each monkey at 1 week and at 1 and 2 months p.i. using methods previously described (22). Chromosomal DNA was prepared from plate-grown cells using the cetyltrimethylammonium bromide method (6). Degenerate oligonucleotide primers (50 pmol each) REP1R-Dt (5′-IIINCGNC GNCATCNGGC-3′) and REP2-Dt (5′-NCGNCTTATCNGGCCTAC-3′) were added to a 25-μl PCR that contained 100 ng of template DNA, 6 mM $MgCl_2$, 0.6 mM concentrations of each deoxynucleoside triphosphates, and 2 units Ampli-*Taq* DNA polymerase (Applied Biosystems, Foster City, CA). Amplification conditions were initial denaturation at 94°C for 2 min, 30 PCR cycles (94°C for 30 s, 45°C for 1 min, and 72°C for 3 min), and a single extension of 72°C for 5 min. PCR products were separated on 1.5% agarose gels, and fragments were visualized by ethidium bromide staining.

Primer design. Gene-specific oligonucleotide primer pairs were utilized from a previous experiment (10), and new ones were designed for additional genes (Table 1) using Oligo 6.0 software (Molecular Biology Insights, Cascade, CO) and the known genome sequences of *H. pylori* 26695 (44) and J99 (3). All primer pairs had a calculated melting temperature of 68 to 70°C, amplified products between 100 to 300 bp, and ended with a double dA 3′ terminus homologous to

the template (36). Every primer pair was first used to amplify DNA from *H. pylori* J166, and the predicted amplicon size was verified by agarose gel electrophoresis prior to RT-PCR.

qRT-PCR. qRT-PCR was performed with gene-specific primer pairs (Table 1) using methods previously described (10). Briefly, RT and PCR were performed in a single 20-μl reaction mixture using the thermostable recombinant *Tth* (r*Tth*) DNA polymerase (Applied Biosystems), which in the presence of $Mn(OAc)_2$ has reverse transcriptase activity and DNA polymerase activity. The RNA template was either 100 ng RNA from in vitro-grown cells or a 1:5 dilution of in vivo RNA. To eliminate PCR carryover contamination, each reaction mixture also included 0.4 U uracil-DNA-glycosylase (New England Biolabs, Beverly, MA). A two-step amplification was performed for 45 cycles at 95°C for 20 s followed by 59.5°C for 1 min. Accumulation of PCR product was detected during each cycle by excitation of SYBR green at 490 nM. Relative fluorescence was characterized by a cycle threshold (C_t) value, which was defined by the crossover point of the kinetic curve with an arbitrary fluorescence level set at 150 relative fluorescence units. The absence of contaminating DNA was examined by performing the RT-PCR with 2.4 mM $MgCl_2$, in which r*Tth* has DNA polymerase but no RT activity. If the observed C_t with RNA template was not at least 2 cycles less than that of the no-template control (water), the primer pair was eliminated from the analysis.

Primer efficiency. Since even primer pairs with 100% homology to their template can amplify with markedly different efficiencies, we first tested primer pairs with *H. pylori* J166 DNA. Assuming there is one DNA copy per cell for each amplified gene, a C_t was determined and used to calculate the primer efficiency. In our laboratory, efficient amplification of 10^5 bacterial cell equivalents of DNA (0.186 ng) yielded a C_t equal to 18.5, which was arbitrarily defined as 97% efficiency. A primer pair with 97% efficiency would give a standard yield equal to $1.94^{18.5}$ copies after 18.5 cycles of PCR. Therefore, cycle efficiency as a function of the C_t observed for each primer pair can be defined as:

$$\text{cycle efficiency} = 1/2(1.94^{18.5})^{1/C_t \text{ observed}}$$

If the observed C_t for a primer pair is 18.5, then the cycle efficiency is 97%; higher C_t values yield lower cycle efficiencies. Only primer pairs with efficiencies of 90% or better were used. Corrected C_t, which takes into account primer efficiency, can be determined from the following equation, where cycle yield = 2 × cycle efficiency:

$$\text{corrected } C_t = \log_2(\text{cycle yield})^{C_t \text{ observed RNA}}$$

Calculation of absolute gene expression in vitro. Copies per cell were calculated based on three factors: (i) a 10-fold change in starting template concentration corresponds to a change in C_t of 3.3 cycles, (ii) the assumption that 100 ng of RNA equals 10^6 *H. pylori* cells, (iii) the empirically derived observation that a C_t of 18.5 corresponds to 1×10^5 copies of starting DNA template (assuming 1 copy on the chromosome). For example, an observed C_t of 18.5 for a primer pair with 97% efficiency is calculated as 0.1 mRNA copies/cell. Since the starting amount of RNA template (100 ng) represents 10^6 bacterial cells, a C_t of 18.5 for RNA indicates 10-fold less starting template per cell than the same C_t observed with DNA, which is performed with 10^5 cell equivalents. Since a 10-fold change in template concentration corresponds (with efficient amplification) to 3.3 cycles ($2^{3.3} = 10$), we calculate absolute gene expression as:

$$\text{mRNA copies/cell} = 2^{15.2 - \text{corrected } C_t \text{ RNA}}$$

We have previously shown that calculation of mRNA copies/cell using C_t corrected for primer efficiency yields values that are essentially identical to those obtained by the more conventional method using standard curves (10).

Calculation of relative gene expression in vivo. Absolute gene expression could not be calculated for in vivo samples because the number of bacterial cells in each sample was unknown. Therefore, to account for differences in bacterial load among animals, all C_t values were normalized to the C_t of *H. pylori* 16S rRNA for each monkey sample. Data were therefore expressed as:

$$\text{relative gene expression} = 2^{(\text{corrected } C_t \text{ 16S rRNA} - \text{corrected } C_t \text{ gene})}$$

RESULTS AND DISCUSSION

Primer efficiency and control samples. All 46 primer pairs amplified *H. pylori* J166 DNA with at least 90% efficiency. Single bands were detected for each primer pair, and the predicted amplicon length was verified on agarose gels (data not shown). No signal was detected when qRT-PCR was performed with control tissue from uninfected primates nor when $Mn(OAc)_2$ was replaced with 2.4 mM $MgCl_2$, in which r*Tth* has DNA polymerase activity but no RT activity (negative control).

In vitro gene expression. (i) Transcript copies/cell at mid-log growth. Calculation of mRNA copies/cell at mid-log-phase growth (15 h; OD_{600}, 1.0) showed that transcript levels of virulence genes varied by 4 orders of magnitude (Fig. 1A), ranging from 0.004 to almost 20 copies/cell. Expression of *ureA* and *ureB* was the highest, with nearly identical amounts of transcript. This was expected, since urease is one of the most abundant proteins found in *H. pylori* (26) and the genes are transcribed on a single operon. Expression levels of *ureG* and *ureI* were approximately 10- and 100-fold lower than that of *ureAB*, respectively. These accessory urease genes are thought to be transcribed on a second operon that consists of *ureIEFGH*. However, the steady-state level of message from individual genes is complex because both the amount and size of mRNAs from this operon are thought to be affected by a pH-dependent posttranscriptional regulatory mechanism (1). Also among the most highly expressed genes were *napA*, *vacA*, and *babA* (*omp28*), the ABO blood group adhesin (5). NapA was originally described as a promoter of neutrophil adhesion to endothelial cells (19). It was subsequently shown to be a multifunctional protein related to bacterioferritins and to the *Escherichia coli* Dps, a nonspecific DNA-binding protein that is induced by environmental stress and probably protects DNA from oxidative damage (9, 13). It seems likely that NapA and VacA, which was shown recently to inhibit *H. pylori*-specific T-lymphocyte activation (21, 41), are both critical for avoiding innate and adaptive host immunity and maintaining chronic infection. Transcript levels for genes on the Cag PAI also varied by more than 4 orders of magnitude (Fig. 1B), ranging from 0.001 (*cag15*) to 22 (*cag25*) copies/cell. There was no apparent relationship between expression level and whether a gene on the PAI is required for CagA tyrosine phosphorylation or induction of IL-8.

(ii) Growth-phase-dependent gene expression. Growth curves for the duplicate *H. pylori* cultures were nearly identical (Fig. 2). Therefore, we combined the C_t values determined independently from each culture to calculate a mean copy/cell (Fig. 2). C_t values for 16S rRNA varied by less than twofold during the growth curve. The change in gene expression during the growth cycle was expressed as a ratio of mRNA copies/cell at each time point relative to that at 6 h. From late-log-phase (18 h; OD_{600}, 1.4) to stationary-phase (23.5 h; OD_{600}, 1.8) growth, most genes (61%) showed a decrease in expression, though expression increased in some cases (15%). Genes with a change in expression of ≥2-fold are listed in Table 2. Of the 7 genes whose expression was induced, most were also found by whole-genome DNA microarray analysis to be induced by entry into stationary-phase growth (43) and by iron starvation (28). Among the induced genes were *napA* and *katA*, which likely play an important role in protection against oxidative DNA damage during starvation or other environmental stress. There was little correspondence between the genes whose expression we found to be reduced during stationary phase and the results from DNA microarray studies (28, 43). This may in part reflect the fact that repressed genes were expressed at a lower level than induced genes (Table 2) and may have been below the level of detection of the DNA microarray.

TABLE 2. Genes whose expression was induced or repressed ≥2-fold from log- to stationary-phase growth in vitro

Gene	No. of transcript copies/cell in[a]:		Fold change[d]
	Log phase[b]	Stationary phase[c]	
Induced genes			
omp11	1.19	7.20	6.0
napA	18.1	36.8	2.0
katA	2.46	6.90	2.8
vacA	3.71	8.17	2.2
cag1	1.39	3.52	2.5
cag21	0.56	2.39	4.3
cagA	1.22	2.48	2.0
Repressed genes			
ureG	0.98	0.12	8.1
ure1	0.28	0.07	4.2
nixA	1.00	0.47	2.2
omp19	2.40	1.09	2.2
feoB	0.04	0.002	17.1
fur	0.04	0.01	6.5
fliI	0.09	0.003	32.5
fliP	0.08	0.002	36.8
flgE	0.10	0.01	14.7
hpaA	0.01	0.002	2.7
comB8	0.10	0.01	8.5
nolK	0.37	0.04	8.5
cag3	0.93	0.04	24.9
cag5	0.79	0.03	27.3
virB11	0.02	0.003	7.2
cag6	0.11	0.02	5.0
cag7	0.09	0.01	16.5
cag8	0.06	0.02	4.2
cag9	1.68	0.06	26.1
cag10	0.37	0.05	7.4
cag14	0.58	0.26	2.2
cag16	0.14	0.01	19.4
cag17	1.11	0.04	30.0
cag18	0.10	0.02	6.7
cag19	1.46	0.68	2.2

[a] Only values above 0.001 were included in the analysis.
[b] Time point 1; 6 h of growth; OD_{600}, 0.2.
[c] Time point 6; 23.5 h of growth; OD_{600}, 1.8.
[d] Relative change between log and stationary phase, calculated as log/stationary for repressed genes and stationary/log for induced genes.

In vivo gene expression. (i) Quantitative culture and Rep-PCR. Two antral biopsy specimens were used to determine quantitative bacterial load from each monkey at 1 week and 1, 2, 3, 4, and 6 months p.i. At 1 week p.i., all 5 monkeys were infected with 5×10^4 to 4×10^7 CFU/g of tissue. However, between 1 and 6 months p.i., only 1 monkey remained infected with a bacterial load that was sufficient for transcript quantitation. This was likely due to the fact that the inoculum was grown from a single colony, whereas we have previously used a mixture of 6 rhesus-passaged J166 strains (39). A mixed inoculum probably contains greater genomic diversity that more efficiently colonizes multiple hosts (23). Similar observations have recently been made with the mouse model (17). Agarose gel electrophoresis of the Rep-PCR products showed that the output strains from each monkey were identical to the input J166 and differed from representative strains of *H. pylori* that are enzootic in socially housed rhesus monkeys at the CNPRC (Fig. 3). These results confirm that our expression data reflect

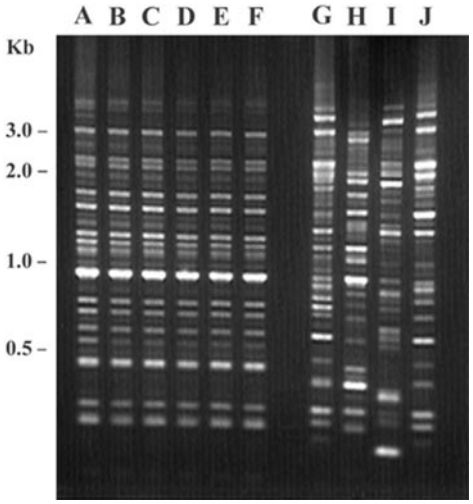

FIG. 3. Agarose gel electrophoresis of Rep-PCR of *H. pylori* input, output, and naturally acquired strains. The output strains are identical to the input strain and can easily be distinguished from other naturally acquired strains. Lane A, *H. pylori* J166 input strain; lanes B to F, five output strains from experimentally infected rhesus monkeys; lanes G to J, naturally acquired rhesus strains of *H. pylori.*

infection with the inoculated strain (J166) and not naturally acquired infection.

To provide an estimate of bacterial load, we normalized the C_t for in vivo expression to that for 16S rRNA. We therefore compared the quantitative culture results to the C_t for 16S rRNA (Fig. 4). The results showed a close correspondence between CFU/g and C_t over a broad range of bacterial load, with a Pearson product correlation coefficient of 0.80. Since quantitative culture of *H. pylori* from gastric biopsy specimens lacks sensitivity, with a detection limit of 10^2 to 10^3 CFU/g of tissue, qRT-PCR can be used as a more accurate measure of infection when bacterial load is low. For genes with high expression levels, it may sometimes be possible to reliably quan-

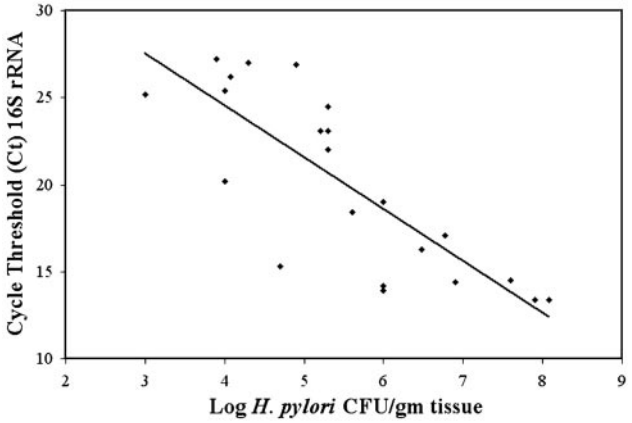

FIG. 4. Comparison of quantitative culture results to C_t for 16S rRNA. Each datum point represents a single animal. For rRNA C_t values, RNA was extracted from 6 combined biopsy specimens. For the CFU/g data, 2 biopsy specimens were combined and cultured. The best fit linear trend line is shown, and the Pearson product correlation coefficient was found to be 0.80 ($P < 0.005$).

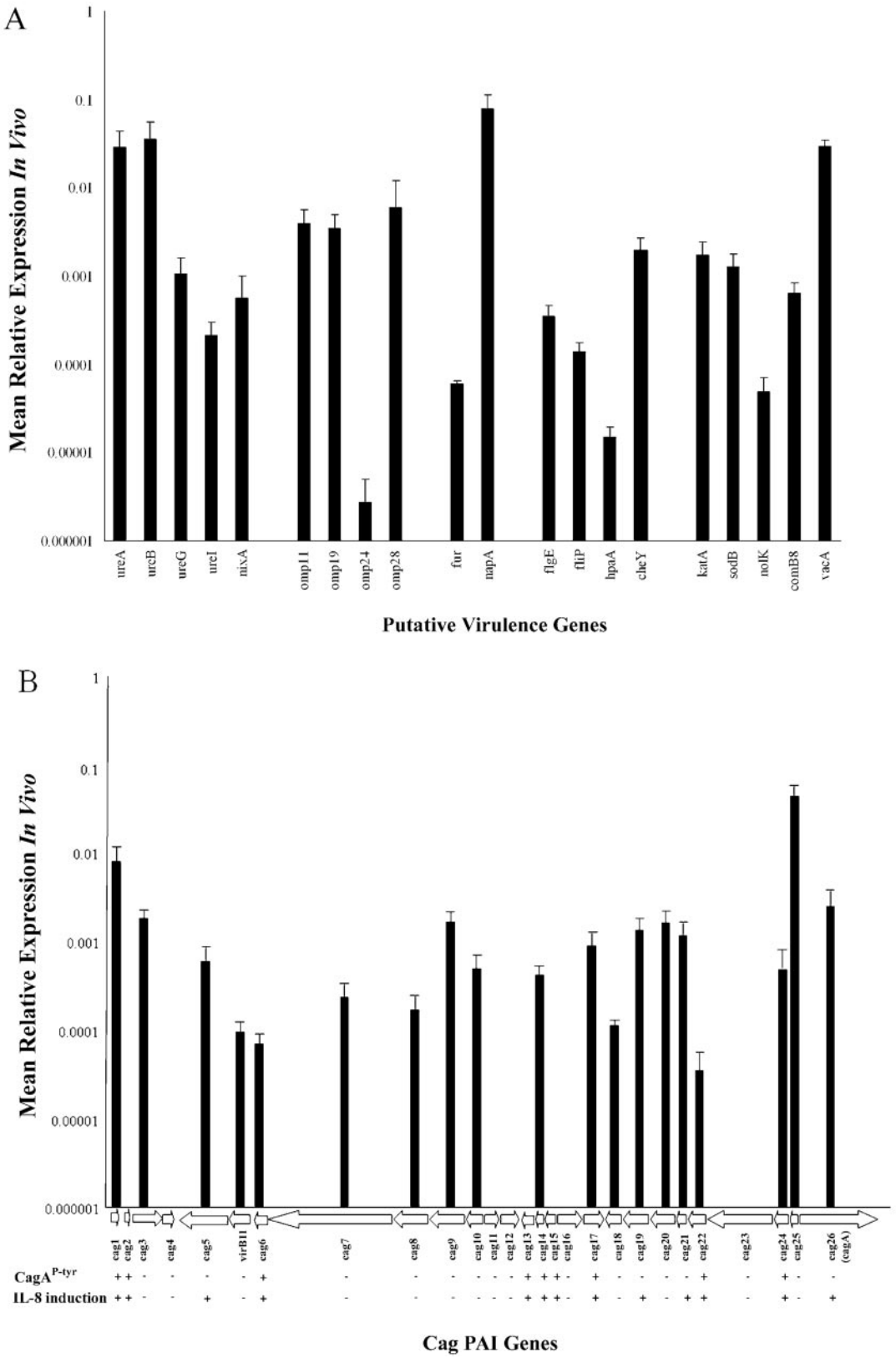

FIG. 5. Relative expression in vivo 1 week p.i. normalized to the level of 16S rRNA (16S rRNA = 1.0). (A) Relative expression levels of putative virulence genes, grouped according to similar functions (Table 1). (B) Relative expression of genes on the Cag PAI. Arrows represent the direction of the open reading frame. Plus and minus signs indicate whether a nonpolar deletion mutant in the respective PAI gene shows the phenotype of IL-8 induction or CagA tyrosine phosphorylation according to published data (20). Genes for which no data are shown were not examined.

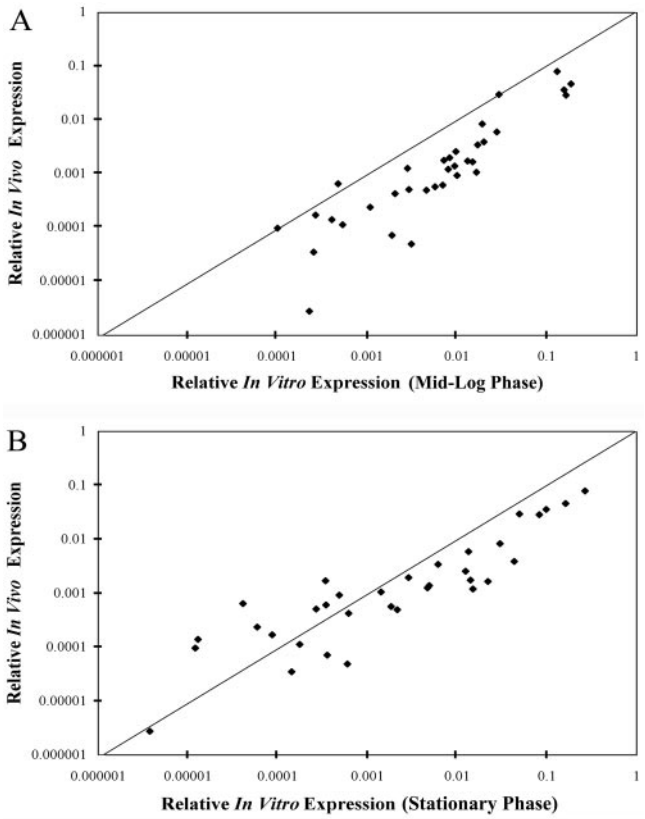

FIG. 6. Dot plot comparing the relative gene expression between in vivo and in vitro samples. Points above the diagonal line represent genes whose expression is higher in vivo, and points below the line are genes whose expression is higher in vitro. In vivo datum points are the averages of the results from 3 to 5 animals, with each gene analyzed in duplicate. In vitro expression was analyzed for duplicate cultures during mid-log-phase growth (15 h; OD_{600}, 1.0) (A) and stationary-phase growth (23.5 h; OD_{600}, 1.8) (B). The Pearson product correlation coefficients were 0.89 and 0.88 for the data shown in panels A and B, respectively.

TABLE 3. Genes whose expression was induced or repressed by ≥2-fold during acute-phase infection in vivo

Gene	Fold change at[a]:		
	1 wk vs 2–3 mo	2–3 mo vs 4–6 mo	1 wk vs 4–6 mo
Induced genes			
omp11	2.1	—[b]	—
omp19	4.8	—	5.0
hpaA	—	2.3	—
sodB	2.4	—	—
vacA	—	—	2.1
cag7	3.9	—	—
cag14	2.3	—	—
cag18	2.0	—	—
cag24	2.0	—	—
Repressed genes			
nixA	—	4.2	5.1
omp28	4.5	—	—
fliP	—	2.0	—
flgE	—	3.5	—
cag6	—	2.2	—
cag7	—	4.5	—
cag11	—	2.1	—
cag17	—	2.2	—
cag25	—	2.3	—

[a] Change (*n*-fold) in relative gene expression.
[b] —, <2-fold change in gene expression.

titate gene expression from biopsy specimens that are negative by culture but which are positive by qRT-PCR for 16S rRNA.

(ii) Relative gene expression at 1 week p.i. To account for differences in bacterial load, all C_t values were normalized to the C_t of 16S rRNA for each animal, which was 1.0 by definition. Since 16S rRNA is more abundant than bacterial message, relative expression ranged from 0 to 1. Expression levels for most genes represent mean data from the results from 5 animals, though in some cases, due to low bacterial load, expression could only be determined from 3 or 4 animals. Relative gene expression of the virulence and Cag PAI genes was between 1 and 5 logs lower than 16S rRNA (Fig. 5A and B). Genes that were highly expressed in vitro, such as *ureA*, *ureB*, *napA*, *cag1*, and *cag25*, were also the most highly expressed genes in vivo. The lowest expression among the Cag PAI genes was *cag22*, which is required for IL-8 induction and CagA translocation (20). This suggests that even expression levels more than 4 orders of magnitude lower than 16S rRNA are biologically relevant.

In vivo versus in vitro gene expression. To identify genes that were induced or repressed in vivo, we first compared expression in vitro at mid-log phase (15 h; OD_{600}, 1.0) to in vivo expression at 1 week p.i. Relative gene expression for the in vitro data was calculated exactly as for the in vivo data (see Materials and Methods). Gene expression was generally lower in vivo compared to in vitro expression during mid-log phase (Fig. 6A). The mean (±standard deviation) ratios of in vivo to in vitro expression during mid-log phase were 0.34 (±0.36) and 0.24 (±0.23) for the virulence and Cag PAI genes, respectively. We next compared in vivo expression at 1 week p.i. to station-

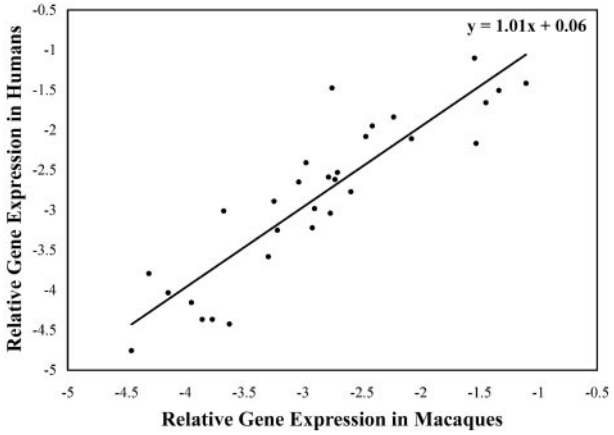

FIG. 7. Comparison of the relative in vivo gene expression in rhesus macaques to that found in humans (determined from previously published data) (10). Data report only genes that are in common between the two studies. The time point for the rhesus macaque data was 1 week p.i., and data represent mean gene expression for results from five animals. Relative gene expression data are plotted as $\log_{10}$. The Pearson product correlation coefficient was calculated to be 0.89. The best fit linear trend line and linear equation are shown.

ary-phase expression (23.5 h; OD_{600}, 1.8) in vitro (Fig. 6B). This analysis showed that 9 genes were more highly expressed in vivo than in vitro (Fig. 6B). Of these, 6 genes (*cag5*, *virB11*, *cag7*, *cag8*, *cag9*, and *cag10*) are found contiguously on the PAI (absent *cag6*), are oriented with open reading frames (ORFs) in the same direction, and are flanked by genes (*cag4* and *cag11*) whose ORFs are in the opposite direction (Fig. 1B). Most of these genes are implicated by experimental analysis (32, 35, 42) or by sequence homology (11) to form portions of the type IV secretion pilus or its accessory proteins. In addition, another gene that appeared induced in vivo (*comB8*) is thought to encode a portion of a second *H. pylori* type IV secretion system that is utilized for DNA uptake and is required for competence (25). These results suggest the possibility that at least some of the genes encoding the *H. pylori* type IV structural pilus and its accessory proteins may form an operon that is induced during growth in vivo.

In vivo gene expression over time. We analyzed in vivo *H. pylori* gene expression for one monkey at 1 week and 2, 3, 4, and 6 months p.i. To simplify the analysis, we grouped the data into early (1 week)-, mid (2 to 3 months)-, and late (4 to 6 months)-acute-phase infection. Interestingly, almost all genes that showed more than a twofold induction were induced during early- to mid-acute-phase infection (between 1 week and 2 to 3 months p.i.) (Table 3). These genes included outer membrane proteins (OMPs), superoxide dismutase, and Cag PAI genes, which may all play a role in establishing the infection and evading the initial host immune response. Early in infection, we saw apparent repression of *babA* (*omp28*), which codes for the ABO blood group binding adhesin (5), and induction of *babB* (*omp19*), a gene encoding for a related OMP with unknown function. However, we recently reported that infection of rhesus macaques with *H. pylori* J166 results in selection for strains that have undergone a gene conversion, whereby *babA* has been deleted and replaced by a duplicated copy of *babB*. Therefore, this apparent change in expression of *H. pylori* OMPs is mediated by genomic recombination and not by regulation of expression in the conventional sense. The apparent changes in *cag7* (*cagY*) expression (Table 3) may also be mediated by genomic events, since *cag7* has extensive repeats that mediate in-frame deletions and duplications (4). These findings emphasize that, particularly in *H. pylori*, apparent changes in expression may sometimes reflect modifications in the genome rather than bacterial sensing of environmental signals via traditional two-component regulatory systems.

Comparison of *H. pylori* gene expression in rhesus macaques and humans. We recently used qRT-PCR to perform *H. pylori* transcription profiling in chronically infected human patients (10). In general, the results are similar to those described here, which further validates the use of the macaque as a model of human infection. The Pearson product correlation coefficient between in vivo gene expression levels in humans and macaques was 0.89 (Fig. 7), and the trend line had a slope of 1.0. This is a striking finding in view of the fact that these data were collected not only from different host species but also from different bacterial strains and at different time periods. The generally reduced expression levels in vivo compared to in vitro also mimics the results seen for humans. We cannot fully exclude the possibility that this finding is spurious. For example, if extraction efficiency for mRNA versus stable RNA is lower in vivo than it is in vitro, we might incorrectly conclude that expression is lower in vivo. If this were the case, the reduced extraction efficiency of mRNA from in vivo samples might be particularly troublesome for low-abundance message, which would lead us to conclude erroneously that reduced expression in vivo was exaggerated for genes with low transcript abundance. However, this is the opposite of what we observed (Fig. 6B). Furthermore, the fact that the result is robust over differences in host and bacterial strains suggests that reduced expression in vivo for many (but not all) genes reflects the biology of *H. pylori* infection and is not an artifact of the methods used here.

These results provide, for the first time, a quantitative fingerprint of *H. pylori* gene expression in vitro and in vivo in experimentally infected nonhuman primates. Comparison of *H. pylori* gene expression in vivo to expression in vitro during stationary phase suggests the possibility that some genes encoding the *H. pylori* type IV structural pilus and accessory proteins may form an operon that is induced during growth in vivo.

ACKNOWLEDGMENTS

We thank Michael Syvanen for many helpful discussions.

This work was supported in part by Public Health Service grants AI42081, RR14298, and RR15293 from the National Institutes of Health.

REFERENCES

1. **Akada, J. K., M. Shirai, H. Takeuchi, M. Tsuda, and T. Nakazawa.** 2000. Identification of the urease operon in Helicobacter pylori and its control by mRNA decay in response to pH. Mol. Microbiol. **36:**1071–1084.
2. **Akopyants, N. S., S. W. Clifton, D. Kersulyte, J. E. Crabtree, B. E. Youree, C. A. Reece, N. O. Bukanov, E. S. Drazek, B. A. Roe, and D. E. Berg.** 1998. Analyses of the cag pathogenicity island of Helicobacter pylori. Mol. Microbiol. **28:**37–53.
3. **Alm, R. A., L. S. Ling, D. T. Moir, B. L. King, E. D. Brown, P. C. Doig, D. R. Smith, B. Noonan, B. C. Guild, B. L. deJonge, G. Carmel, P. J. Tummino, A. Caruso, M. Uria-Nickelsen, D. M. Mills, C. Ives, R. Gibson, D. Merberg, S. D. Mills, Q. Jiang, D. E. Taylor, G. F. Vovis, and T. J. Trust.** 1999. Genomic-sequence comparison of two unrelated isolates of the human gastric pathogen Helicobacter pylori. Nature **397:**176–180.
4. **Aras, R. A., W. Fischer, G. I. Perez-Perez, M. Crosatti, T. Ando, R. Haas, and M. J. Blaser.** 2003. Plasticity of repetitive DNA sequences within a bacterial (type IV) secretion system component. J. Exp. Med. **198:**1349–1360.
5. **Aspholm-Hurtig, M., G. Dailide, M. Lahmann, A. Kalia, D. Ilver, N. Roche, S. Vikstrom, R. Sjostrom, S. Linden, A. Backstrom, C. Lundberg, A. Arnqvist, J. Mahdavi, U. J. Nilsson, B. Velapatino, R. H. Gilman, M. Gerhard, T. Alarcon, M. Lopez-Brea, T. Nakazawa, J. G. Fox, P. Correa, M. G. Dominguez-Bello, G. I. Perez-Perez, M. J. Blaser, S. Normark, I. Carlstedt, S. Oscarson, S. Teneberg, D. E. Berg, and T. Boren.** 2004. Functional adaptation of BabA, the H. pylori ABO blood group antigen binding adhesin. Science **305:**519–522.
6. **Ausubel, F. M.** 1988. Current protocols in molecular biology. John Wiley & Sons, New York, N.Y.
7. **Backert, S., T. Schwarz, S. Miehlke, C. Kirsch, C. Sommer, T. Kwok, M. Gerhard, U. B. Goebel, N. Lehn, W. Koenig, and T. F. Meyer.** 2004. Functional analysis of the *cag* pathogenicity island in *Helicobacter pylori* isolates from patients with gastritis, peptic ulcer, and gastric cancer. Infect. Immun. **72:**1043–1056.
8. **Backert, S., E. Ziska, V. Brinkmann, U. Zimny-Arndt, A. Fauconnier, P. R. Jungblut, M. Naumann, and T. F. Meyer.** 2000. Translocation of the Helicobacter pylori CagA protein in gastric epithelial cells by a type IV secretion apparatus. Cell. Microbiol. **2:**155–164.
9. **Barnard, F. M., M. F. Loughlin, H. P. Fainberg, M. P. Messenger, D. W. Ussery, P. Williams, and P. J. Jenks.** 2004. Global regulation of virulence and the stress response by CsrA in the highly adapted human gastric pathogen Helicobacter pylori. Mol. Microbiol. **51:**15–32.
10. **Boonjakuakul, J. K., M. Syvanen, A. Suryaprasad, C. L. Bowlus, and J. V. Solnick.** 2004. Transcription profile of Helicobacter pylori in the human stomach reflects its physiology in vivo. J. Infect. Dis. **190:**946–956.
11. **Camilli, A., D. T. Beattie, and J. J. Mekalanos.** 1994. Use of genetic recombination as a reporter of gene expression. Proc. Natl. Acad. Sci. USA **91:** 2634–2638.

12. **Censini, S., C. Lange, Z. Xiang, J. E. Crabtree, P. Ghiara, M. Borodovsky, R. Rappuoli, and A. Covacci.** 1996. Cag, a pathogenicity island of Helicobacter pylori, encodes type I-specific and disease-associated virulence factors. Proc. Natl. Acad. Sci. USA **93:**14648–14653.
13. **Cooksley, C., P. J. Jenks, A. Green, A. Cockayne, R. P. Logan, and K. R. Hardie.** 2003. NapA protects Helicobacter pylori from oxidative stress damage, and its production is influenced by the ferric uptake regulator. J. Med. Microbiol. **52:**461–469.
14. **Drazek, E. S., A. Dubois, and R. K. Holmes.** 1994. Characterization and presumptive identification of Helicobacter pylori isolates from rhesus monkeys. J. Clin. Microbiol. **32:**1799–1804.
15. **Dubois, A., D. E. Berg, E. T. Incecik, N. Fiala, L. M. Heman-Ackah, G. I. Perez-Perez, and M. J. Blaser.** 1996. Transient and persistent experimental infection of nonhuman primates with *Helicobacter pylori*: implications for human disease. Infect. Immun. **64:**2885–2891.
16. **Dubois, A., N. Fiala, L. M. Heman-Ackah, E. S. Drazek, A. Tarnawski, W. N. Fishbein, G. I. Perez-Perez, and M. J. Blaser.** 1994. Natural gastric infection with Helicobacter pylori in monkeys: a model for spiral bacteria infection in humans. Gastroenterology **106:**1405–1417.
17. **Eaton, K.** Abstr. 104th Gen. Meet. Am. Soc. Microbiol., abstr. D-213, 2004.
18. **Eaton, K. A., C. L. Brooks, D. R. Morgan, and S. Krakowka.** 1991. Essential role of urease in pathogenesis of gastritis induced by *Helicobacter pylori* in gnotobiotic piglets. Infect. Immun. **59:**2470–2475.
19. **Evans, D. J., Jr., D. G. Evans, T. Takemura, H. Nakano, H. C. Lampert, D. Y. Graham, D. N. Granger, and P. R. Kvietys.** 1995. Characterization of a *Helicobacter pylori* neutrophil-activating protein. Infect. Immun. **63:**2213–2220.
20. **Fischer, W., J. Puls, R. Buhrdorf, B. Gebert, S. Odenbreit, and R. Haas.** 2001. Systematic mutagenesis of the Helicobacter pylori cag pathogenicity island: essential genes for CagA translocation in host cells and induction of interleukin-8. Mol. Microbiol. **42:**1337–1348.
21. **Gebert, B., W. Fischer, E. Weiss, R. Hoffmann, and R. Haas.** 2003. Helicobacter pylori vacuolating cytotoxin inhibits T lymphocyte activation. Science **301:**1099–1102.
22. **Go, M. F., K. Y. Chan, J. Versalovic, T. Koeuth, D. Y. Graham, and J. R. Lupski.** 1995. Cluster analysis of Helicobacter pylori genomic DNA fingerprints suggests gastroduodenal disease-specific associations. Scand. J. Gastroenterol. **30:**640–646.
23. **Hansen, L. M., and J. V. Solnick.** 2001. Selection for urease activity during *Helicobacter pylori* infection of rhesus macaques (*Macaca mulatta*). Infect. Immun. **69:**3519–3522.
24. **Higashi, H., R. Tsutsumi, S. Muto, T. Sugiyama, T. Azuma, M. Asaka, and M. Hatakeyama.** 2002. SHP-2 tyrosine phosphatase as an intracellular target of Helicobacter pylori CagA protein. Science **295:**683–686.
25. **Hofreuter, D., S. Odenbreit, and R. Haas.** 2001. Natural transformation competence in Helicobacter pylori is mediated by the basic components of a type IV secretion system. Mol. Microbiol. **41:**379–391.
26. **Hu, L. T., and H. L. Mobley.** 1990. Purification and N-terminal analysis of urease from *Helicobacter pylori*. Infect. Immun. **58:**992–998.
27. **Inui, T., S. Mizuno, K. Takai, M. Nakagawa, M. Uchida, M. Fujimiya, A. Asakawa, and A. Inui.** 2003. Helicobacter pylori cytotoxin: a novel ligand for receptor-like protein tyrosine phosphatase beta. Int. J. Mol. Med. **12:**917–921.
28. **Merrell, D. S., L. J. Thompson, C. C. Kim, H. Mitchell, L. S. Tompkins, A. Lee, and S. Falkow.** 2003. Growth phase-dependent response of *Helicobacter pylori* to iron starvation. Infect. Immun. **71:**6510–6525.
29. **Odenbreit, S., J. Puls, B. Sedlmaier, E. Gerland, W. Fischer, and R. Haas.** 2000. Translocation of Helicobacter pylori CagA into gastric epithelial cells by type IV secretion. Science **287:**1497–1500.
30. **O'Rourke, J. L., J. V. Solnick, B. A. Neilan, K. Seidel, R. Hayter, L. M. Hansen, and A. Lee.** 2004. Description of 'Candidatus Helicobacter heilmannii' based on DNA sequence analysis of 16S rRNA and urease genes. Int. J. Syst. Evol. Microbiol. **54:**2203–2211.
31. **Ottemann, K. M., and A. C. Lowenthal.** 2002. *Helicobacter pylori* uses motility for initial colonization and to attain robust infection. Infect. Immun. **70:**1984–1990.
32. **Rohde, M., J. Puls, R. Buhrdorf, W. Fischer, and R. Haas.** 2003. A novel sheathed surface organelle of the Helicobacter pylori cag type IV secretion system. Mol. Microbiol. **49:**219–234.
33. **Segal, E. D., J. Cha, J. Lo, S. Falkow, and L. S. Tompkins.** 1999. Altered states: involvement of phosphorylated CagA in the induction of host cellular growth changes by Helicobacter pylori. Proc. Natl. Acad. Sci. USA **96:**14559–14564.
34. **Segal, E. D., S. Falkow, and L. S. Tompkins.** 1996. Helicobacter pylori attachment to gastric cells induces cytoskeletal rearrangements and tyrosine phosphorylation of host cell proteins. Proc. Natl. Acad. Sci. USA **93:**1259–1264.
35. **Selbach, M., S. Moese, T. F. Meyer, and S. Backert.** 2002. Functional analysis of the *Helicobacter pylori cag* pathogenicity island reveals both VirD4-CagA-dependent and VirD4-CagA-independent mechanisms. Infect. Immun. **70:**665–671.
36. **Sninsky, J. J., M. A. Innis, and D. H. Gelfand.** 1999. PCR applications: protocols for functional genomics. Academic Press, San Diego, Calif.
37. **Solnick, J. V., D. R. Canfield, S. Yang, and J. Parsonnet.** 1999. Rhesus monkey (Macaca mulatta) model of Helicobacter pylori: noninvasive detection and derivation of specific-pathogen-free monkeys. Lab. Anim. Sci. **49:**197–201.
38. **Solnick, J. V., K. Chang, D. R. Canfield, and J. Parsonnet.** 2003. Natural acquisition of *Helicobacter pylori* infection in newborn rhesus macaques. J. Clin. Microbiol. **41:**5511–5516.
39. **Solnick, J. V., L. M. Hansen, D. R. Canfield, and J. Parsonnet.** 2001. Determination of the infectious dose of *Helicobacter pylori* during primary and secondary infection in rhesus monkeys (*Macaca mulatta*). Infect. Immun. **69:**6887–6892.
40. **Suerbaum, S., and P. Michetti.** 2002. Helicobacter pylori infection. N. Engl. J. Med. **347:**1175–1186.
41. **Sundrud, M. S., V. J. Torres, D. Unutmaz, and T. L. Cover.** 2004. Inhibition of primary human T cell proliferation by Helicobacter pylori vacuolating toxin (VacA) is independent of VacA effects on IL-2 secretion. Proc. Natl. Acad. Sci. USA **101:**7727–7732.
42. **Tanaka, J., T. Suzuki, H. Mimuro, and C. Sasakawa.** 2003. Structural definition on the surface of Helicobacter pylori type IV secretion apparatus. Cell. Microbiol. **5:**395–404.
43. **Thompson, L. J., D. S. Merrell, B. A. Neilan, H. Mitchell, A. Lee, and S. Falkow.** 2003. Gene expression profiling of *Helicobacter pylori* reveals a growth-phase-dependent switch in virulence gene expression. Infect. Immun. **71:**2643–2655.
44. **Tomb, J. F., O. White, A. R. Kerlavage, R. A. Clayton, G. G. Sutton, R. D. Fleischmann, K. A. Ketchum, H. P. Klenk, S. Gill, B. A. Dougherty, K. Nelson, J. Quackenbush, L. Zhou, E. F. Kirkness, S. Peterson, B. Loftus, D. Richardson, R. Dodson, H. G. Khalak, A. Glodek, K. McKenney, L. M. Fitzegerald, N. Lee, M. D. Adams, J. C. Venter, et al.** 1997. The complete genome sequence of the gastric pathogen Helicobacter pylori. Nature **388:**539–547.
45. **van der Woude, M. W., and A. J. Baumler.** 2004. Phase and antigenic variation in bacteria. Clin. Microbiol. Rev. **17:**581–611.

Editor: V. J. DiRita